

Article

# GIS-Based Visibility Network and Defensibility Model to Reconstruct Defensive System of the Han Dynasty in Central Xinjiang, China

Jianfeng Zhu <sup>1,2</sup> , Yueping Nie <sup>1,2</sup>, Huaguang Gao <sup>2,3</sup>, Fang Liu <sup>1,2</sup> and Lijun Yu <sup>1,2,\*</sup>

<sup>1</sup> Institute of Remote Sensing and Digital Earth (RADI), Chinese Academy of Science (CAS), Beijing 100101, China; zhujf@radi.ac.cn (J.Z.); nieyp@radi.ac.cn (Y.N.); liufang115@mailsucas.ac.cn (F.L.)

<sup>2</sup> Joint Laboratory of Remote Sensing Archaeology, Beijing 100101, China; gaohuaguang@163.com

<sup>3</sup> National Museum of China, Beijing 100006, China

\* Correspondence: yulj@radi.ac.cn; Tel.: +86-10-6485-8122

Received: 25 June 2017; Accepted: 10 August 2017; Published: 13 August 2017

**Abstract:** The Silk Road opened during the Han Dynasty, and is significant in global cultural communication. Along this route in the central part of Xinjiang, the archaeological sites with defensive characteristics once provided a safeguard for this area. Reconstructing the defensive system is an important way to explore the ancient culture's propagation and the organizational structure of these sites. In this research, the compound visibility network with complex network analysis (CNA) and the least-cost paths based on the defensibility models from linear and logistic regression methods constitute the principle defensive structure. As possible transportation corridors, these paths are considered to be mostly fitted to each other in general, and are different from normal slope-based paths. The sites Kuhne Shahr and Agra play important roles for information control according to the CNA measures, while the sites Kuhne Shahr and Kuyux Shahr are considered to be crucial cities due to their positions and structural shapes. Some other sites, including Uzgen Bulak, Shah Kalandar, Chuck Castle, Caladar, and Qiuci, as well as some beacons, have important effects on defending the transportation corridors. This method is proven efficient for the study of the historical role of archaeological sites with defensive characteristics.

**Keywords:** defense system; visibility network; defensibility model; regression analysis; least-cost path; transportation corridor

## 1. Introduction

The Silk Road has been an influential cultural path for communication in economy, politics, civilization, and many other aspects since it was opened during the Han Dynasty, after Zhang Qian was sent on a diplomatic mission to the Western Regions (west of Yumenguan, including today's Xinjiang and parts of Central Asia) in 138 B.C. To defend against invasion and maintain political governance, a battery of military fortifications, including the Western Region's Frontier Command, were established at that time. They are considered to be parts of the corporate defensive system to protect the Silk Road [1,2]. Among the discovered relics of ancient fortifications, the city sites were mostly used for expending cultivated land and the population, while the beacons were for safety surveillance and signal transmission [3–5]. Their location preference is related to the intrinsic characteristics for military defense. Therefore, the reconstruction of the defensive system in the Han Dynasty is a critical means to explaining the ancient organizational structure of the remaining archaeological sites and their cultural connotation along the Silk Road.

The distribution of ancient sites is the result of human preference as well as complex decision-making processes. From a military perspective, the ancient sites observed some spatial

regularities to constitute a well-organized system. As an important social organization form, the visibility network can indicate defensive structure among sites [6,7]. Through visibility analysis, some archaeological characteristics and defensive roles can be explored [8–10]. However, it cannot explain the spatial defensibility in the landscape with special preference to build defensive sites. While the defensibility model itself is an effective way to solve this problem (e.g., some defensive indexes are used to build simple models with some possible influencing factors [11,12]), however, with the drawback that the methods of choosing variables and defining their coefficients in the equation are strongly subjective. A more precise model of spatial defensibility is necessary. The spatial distribution characteristics for building an archaeological prediction model could provide references, but most of them put more emphasis on the geographical or environmental aspects (slope, aspect, distance to water, elevation, etc.) in the location analysis under environmental determinism, and some spatial relations of archaeological sites are successfully discovered [13–16]. Other intrinsic factors, such as political, economic, or military considerations, also contribute to the location decision, but they are difficult to quantify [17–21]. The studies are rare on building a defensibility model with quantified military variables. As a matter of fact, the comprehensive analysis of a visibility network and a precisely-qualified defensibility model could help to explain the ancient defensive considerations [22–24].

This study reconstructed a defensive system with a compounded visibility network and defensibility models to speculate the cultural linkage behind military purpose. The transportation corridors based on least-cost analysis of defensibility models were calculated to simulate military and cultural routes during the Han Dynasty along the Silk Road. The organizational structure and historical roles of the archaeological sites were explored, focusing on the observation network and along the transportation routes.

## 2. Study Area and Historical Background

The study area is located in the southern foothills of the Tianshan Mountains and the northern fringe of the Tarim basin with 135,744 km<sup>2</sup> of total area, combining with ten counties from Eastern Yuli to Western Bytown and Xinhe (see Figure 1), of which the latitude is from 39.7° N to 43.1° N and longitude from 84.4° E to 90.4° E. This area has an arid climate but rich water resources. It contains three main types of landforms: the mountainous region, the desert area, and the piedmont alluvial plain. Luntai County, situated in the center, is documented as the location of Western Region's Frontier Command. Ninety-four archaeological sites in the Han Dynasty are located there, including twenty-four city sites, twenty beacon towers, thirty-five tombs, and fifteen general relics that contain a stone inscription, some Buddhist temples, irrigation ditches, smelting relics, and so on.

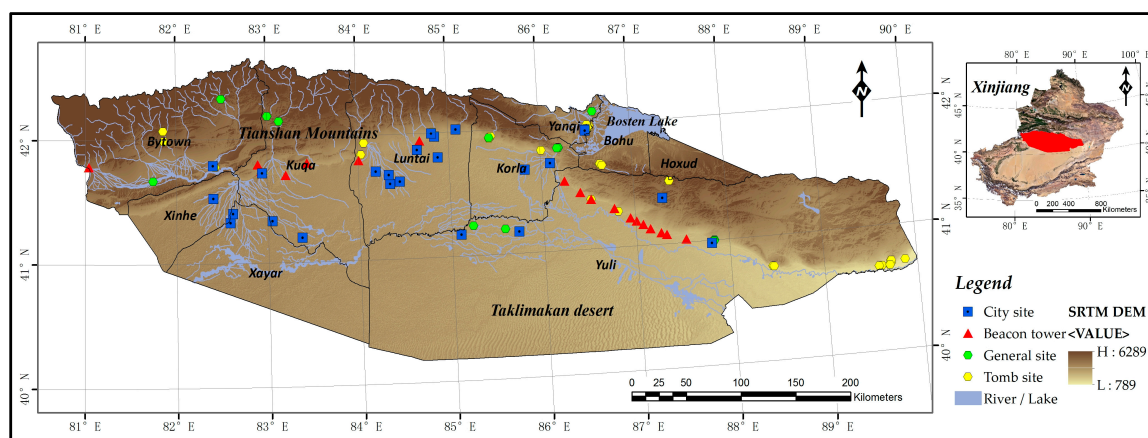


Figure 1. Site distribution of Han Dynasty in the study area.

This area has a famous history and played a crucial role in cultural communication between China and Central Asia, as well as the European continent, after the Silk Road opened. Since 133 B.C., the Han Empire had taken several large-scale military actions to fight against the North Huns. In 101 B.C. (the fourth year of Taichu reign by Emperor Wudi in Han Dynasty), Quli, in today's Yuli County [25,26], and Luntai were chosen to set up the first military fortress to begin populating wasteland and garrisoning the border region [1]. In 60 B.C. (the second year of the Shenjue reign period of Emperor Xuandi of the Han Dynasty), the Western Region's Frontier Command was established to guard the north route (after 1 D.C. of the Emperor Pingdi period, it was called the central path due to a new passageway constructed further north [1]) of the Silk Road [27,28]. Until the Later Han Dynasty, the governed territory changed repeatedly and the Silk Road was closed three different times. The garrison command once moved to Qiuci City, in the current Kuqa County [29]. The geospatial distribution of existing relics can reveal the history during this period.

### 3. Methodology and Results

#### 3.1. Data Collection

DEM (Digital Elevation Model) imagery is necessary for a spatial analysis of archaeological sites. Using a lower spatial resolution of 90 m, SRTM (Shuttle Radar Topography Mission) DEM can provide acceptable average accuracy for this study, in contrast to ASTER GDEM (Advanced Spaceborne Thermal Emission and Reflection Radiometer Global Digital Elevation Model) which has a higher resolution of 30 m but whose elevation values contain severe systematic errors, producing faulty results for visibility analysis in some areas [30]. The initial data of the archaeological sites are from the third cultural relic census, which are recorded with coordinates and attributive descriptions by field survey. For the purposes of this study, the sequence numbers of some important archaeological sites are defined as in Table A1.

#### 3.2. Visibility Analysis

Different types of sites that command the field of view in special directions or which are visible from much of the surrounding territory have been an important part of an ancient defensive system and are of particular note suggested in the context of military or cultural monuments [31]. In order to survey the inter-relation of the defensive system in this study area of the Han Dynasty, point-to-point visibility analysis was employed in ArcGIS 10.2. The recognition of the defensive system was firstly constructed through a compound visibility network combined with visibility lines across the DEM grid surface. It focused especially on the respective monitoring patterns of city sites and beacon towers, which constitute the organizational structure and control over the surrounding territory in different ways. The preconditions to constructing visibility lines observe the following rules:

- The city sites and beacon towers had obvious military function when being built. The tombs with almost no defensive role were ignored during visibility analysis in this research. The general relics—as the related part of city sites—were viewed of no observing function, but observed status in the defensive system.
- According to the documentation and description of the remaining height, the average offset value of the city sites and general relics was assumed as 8 m, and the beacon tower as 12 m.
- The beacon fire—as the signal for military watching and information transmitting—was defined as another 8 m in height. Therefore, the target offset value of an observed beacon is the sum of the tower and its fire height when calculating the visibility line from any site (see Table 1).

**Table 1.** Observing offset in the visibility analysis. B: Beacon tower; C: City site; R: General relic.

Observation Direction	B to B	B to C	B to R	C to C	C to B
Offset A	12	12	12	8	8
Offset B	20	8	8	8	20

The arid environment in this study area provides good observation conditions between sites, excluding meteorological limitations. Nevertheless, the influence of the Earth’s curvature and the border effect should be considered in the visibility analysis. The global visibility network (Figure 2) was combined with an individual visibility line connecting C23 to C24 and three divided local networks.

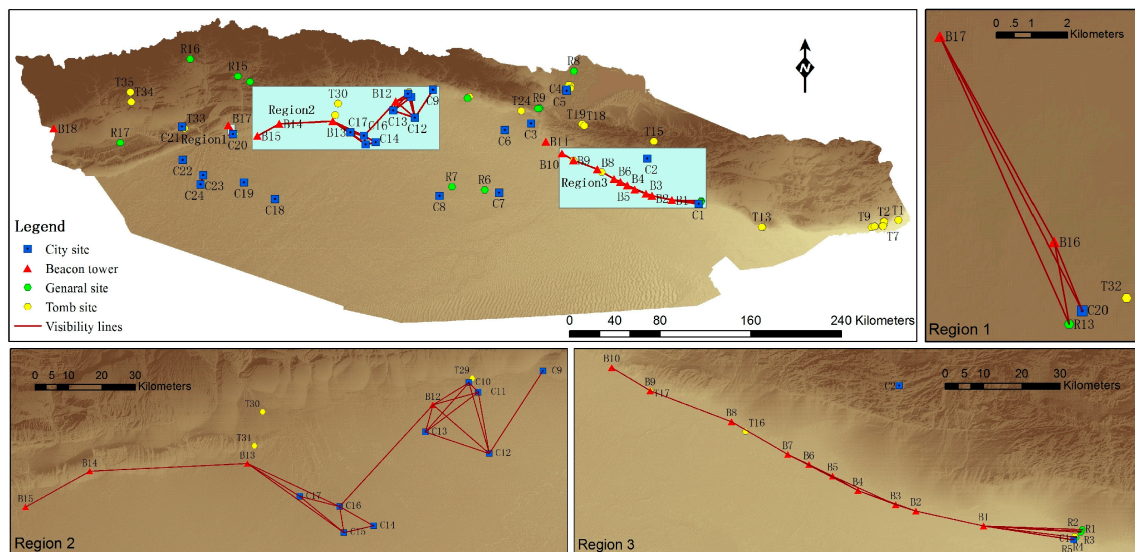


**Figure 2.** Visibility network for military defense in the Han Dynasty. It is combined with lines of sight and defense related sites, including city sites, beacon towers and general sites.

Complex network analysis (CNA) is a mathematical form of graph theory used to characterize network structure and find the different importances of nodes. As a formalized methodology, it delineates the social character of the visibility network among the archaeological sites [32–34], including how defensibility is organized through the nodes (archaeological sites) and links (visibility lines) in the local region, and how important the sites are by the different measures in Table 2.

**Table 2.** The complex network analysis (CNA) measures in the visibility network [35–37].

Density <sup>a</sup>	Inclusivity <sup>a</sup>	Degree <sup>b</sup>	Betweenness <sup>b</sup>	Closeness <sup>b</sup>
$\frac{2 \cdot m}{n \cdot (n-1)}$	$\frac{v}{n}$	$j$	$\sum_{s \neq i \neq t \in N} \frac{\sigma_{st}(i)}{\sigma_{st}}$	$\frac{1}{\sum_{j \neq i \in N} d_j(i)}$
$m$ : number of visibility lines; $n$ : number of all nodes.	$v$ : number of visible nodes; $n$ : number of all nodes.	$j$ : number of connecting lines at the node $i$ .	$\sigma_{st}(i)$ : number of shortest paths from node $s$ to $t$ via node $i$ ; $\sigma_{st}$ : number of the shortest paths from node $s$ to $t$ .	$d_j(i)$ : hops of the shortest paths from the node $i$ to node $j$ .

<sup>a</sup> Global measures; <sup>b</sup> Node-scale measures.

- The density is defined as the ratio of actual connections of visibility lines to potential connections, implicating integral redundancy or multi-path transmission of the information. The value closer to one represents more redundancy than that approaching zero.

- Inclusivity is another measurement of network density. It is defined as the proportion of visible nodes in the whole network. The value approximating one means a less isolated and more organized network.
- The degree is introduced to quantify the number of nodes connected by visibility lines within one hop at the given node, referring to the local connectivity and the centrality of a node in the network.
- Betweenness that scales with the number of pairs of nodes as implied by the summation indices is used to describe the degree of governmental control over the information exchange at the given node. It is suitable for detecting critical nodes and crossroads in the network.
- Closeness is a length measure which is calculated as the sum of the shortest paths from a given node to all the others in the network. Thus, a small value of a given node means it has a central position to all.

The global CNA measures in Table 3 show a higher density and inclusivity of Region 2 and Region 3. In addition, each site is described with three indicators in both scatter and bubble forms in Figure 3.

**Table 3.** CNA measures of global visibility network.

	Region 1	Region 2	Region 3
Density	0.003	0.014	0.013
Inclusivity	0.070	0.228	0.281

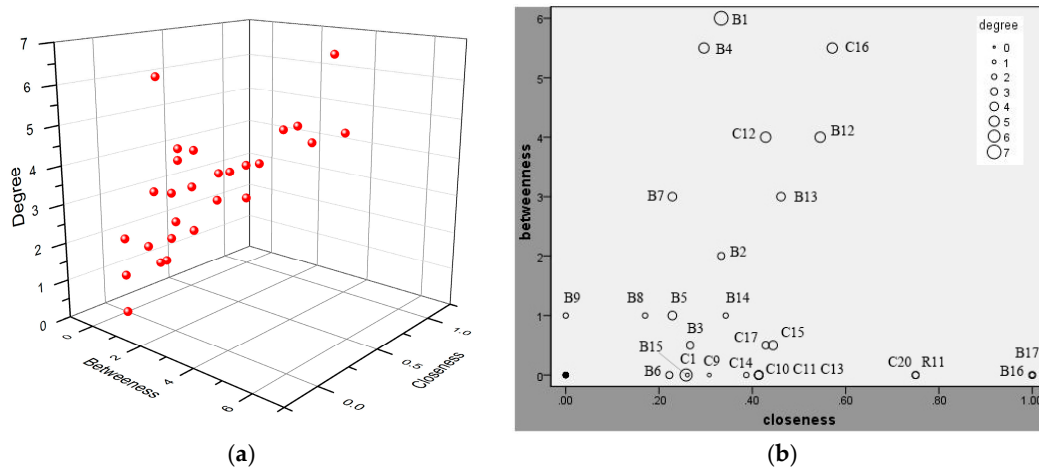


**Figure 3.** (a) Scatter plot and (b) bubble plot of node-scale CNA measures (degree, betweenness, and closeness).

### 3.3. Defensibility Models

#### 3.3.1. Interpretation of Possible Variables

Quantified defensibility could not only explain the relative importance of every site and the landscape, but also reveal the cultural communication pattern between different regions in sociology and anthropology and its influencing factors [21,34]. The independent variables selection is crucial when building a defensibility model. The geographical factors are mostly utilized for spatial analysis and location prediction in archaeological models [38], and they are also considered as valid variables in this defensibility model, in association with other defense-related factors [39,40]. The defensibility was delineated with ten independent variables by GIS tools: proximity to road network, proximity to water, cumulative viewshed from cities and from beacons, density of visibility lines, density of

sites, distance to city, distance to beacon, as well as the geographical factors of slope and elevation. In particular, the first two variables mentioned are inversely proportional to defensive requirements. All variables were normalized before entering a model to remove the impact of different units when judging the importance by the coefficient value of a variable. The defensibility model was built with linear regression and logistic regression analysis, respectively.

### 3.3.2. Linear Regression Analysis

Linear regression analysis can describe most of the issues with causalities, in practice [41]. As for the dependent variable, the relative importance (RI) of a landscape is not a directly observable value, but can be described with weighted and classified indexes. The definition is expressed in the following formula:

$$RI = P_i \cdot A_i \quad (1)$$

where  $A_i$  is the area of an archaeological site, and  $P_i$  is the importance of an ancient site according to the protection level, as defined by the national cultural relics department (national level: 4; provincial level: 3; municipal or prefectural level: 2; unidentified level: 1). The RI grade of these ninety-four archaeological sites was classified into four ranges according to the defensive contribution of each archaeological type as in Table 4, and defined as four corresponding grade values as in Figure 4. The relative importance of a site was used to describe its surrounding landscape in this linear model. The higher the importance grade of a site, the more defensibility is required in the landscape.

**Table 4.** Classification of relative importance in the defensive system. The importance is ranked in four ranges by the sequence of city, beacon, general relics, and tomb according to the defensive contribution, and then each archaeological type is classified into four grades.

	City	Beacon	General Relic	Tomb
Classified grade	7–10	5–8	3–6	1–4

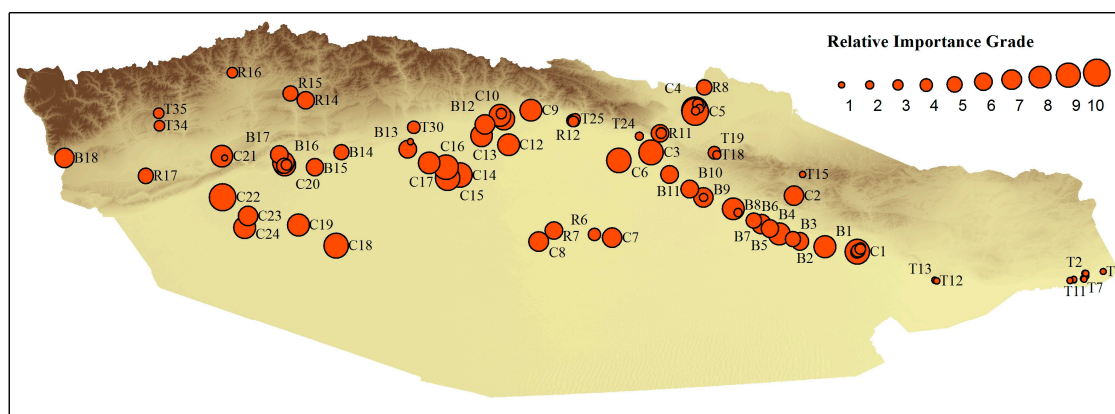


**Figure 4.** Definition of relative importance grade based on defensive function and site area.

A backward regression method was used in linear model building. All the independent variables were entered into the initial model, and then the one with a minimum correlation to the dependent variables was deleted first. The remaining variables repeated this step in the updating model until no independent variables could be eliminated. Four variables were chosen in the final model, where three had a positive effect on the defensibility and only the slope variable had negative impact (in Table 5). The statistical results are shown in Table 6. An adjusted  $R^2$  value of 0.427 represents about 42.7% of defensive importance explainable in this model. The Koenker (BP) and robust probability (Robust\_Pr) were statistically significant, meaning that all the coefficients were significant to represent an actual relationship between each explanatory variable and the dependent variable. The Wald

statistic significance means that this overall model is statistically acceptable. If the variance inflation factors (VIF) are small in the result, it indicates less redundancy among the explanatory variables (when  $VIF < 7.5$ ). With the Jarque-Bera statistic rejecting the significance test, predictions were unbiased and the residuals were normally distributed. All the statistical results proved that the performance in this model was robust and significant. The final defensive importance in the landscape is normalized in Figure 5.

**Table 5.** Independent variables statistical results. Robust\_Pr: robust probability; VIF: variance inflation factor.

Variables	Intercept	ProxtoRoad	DistoCity	Slope	Line_Den
Coefficient	−16.928	18.183	5.022	−7.745	3.221
Probability	0.002 *	0.001 *	0.000 *	0.046 *	0.020 *
Robust_Pr	0.001 *	0.001 *	0.000 *	0.000 *	0.010 *
VIF	–	1.119	1.175	1.059	1.332

\* An asterisk indicates a statistically significant  $p$ -value ( $p < 0.05$ ).

**Table 6.** Overall model statistic results.

Number of Observations	94	(AICc)	416.186
Multiple R-Squared	0.452	Adjusted R-Squared	0.427
Joint F-Statistic	0.000 *	Koenker (BP) Statistic	0.011 *
Joint Wald Statistic	0.000 *	Jarque-Bera Statistic	0.755

\* An asterisk indicates a statistically significant  $p$ -value ( $p < 0.05$ ). AICc: corrected Akaike information criterion.

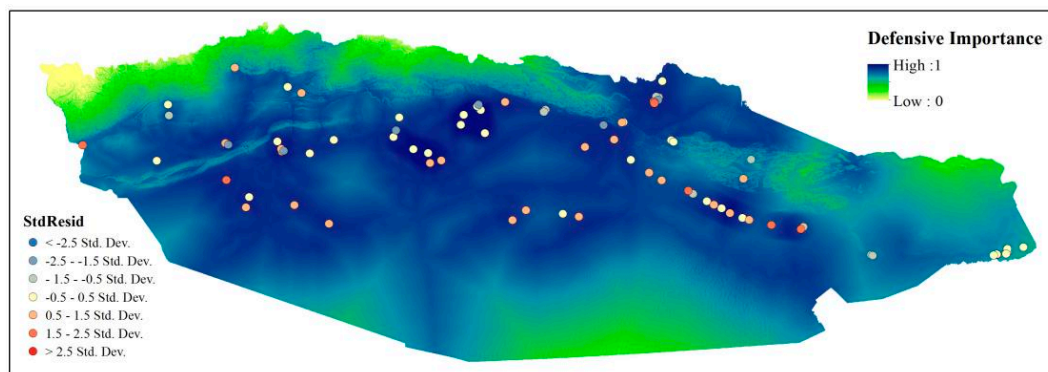


**Figure 5.** Linear regression of defensive importance in the Han Dynasty.

### 3.3.3. Logistic Regression Analysis

The logistic regression analysis was mostly used to delineate the probability of predicting the location of an archaeological site by a binary dependent variable (0: nonoccurrence; 1: occurrence) and independent variables that affect event occurrence [42–44]. In this research, the incident occurrence of an archaeological site being located in a landscape (marked as  $\{y = 1\}$ ) and independent variables  $X_j$  related to defensive factors are expressed as below:

$$P(y = 1) = \frac{1}{1 + e^{-z_k}}, \quad (2)$$

$$z_k = \beta_0 + \sum_j \beta_j \cdot x_{jk} + \varepsilon_k, \quad (3)$$

where variable  $\beta_0$  and regression coefficients  $\beta_j$  reflect the impact of independent variables  $X_j$  on an incident of  $P(y = 1)$ . Furthermore, the presupposition of building a logistic model is that the

relationship between independent and dependent variables is non-linear, whereas the union exponent  $Z_k$  is a linear combination in the hypothetical function.

The observation groups are set as that Group 1 with ninety-four archaeological sites and Group 0 with ninety-four non-site random points. Forward stepwise regression (Likelihood Ratio) is a classic variable selection method that stipulates the criteria of a variable entering into the model that its statistical probability value of likelihood ratio should be less than the given significant level in partial quasi-maximum likelihood estimation. For the overall model, the Cox & Snell  $R^2$  test value was 0.410 (>0.4 best), and Nagelkerke  $R^2$  test value was 0.547 (>0.5 best). Another important indicator—the Hosmer–Lemeshow estimation (Chi-square = 17.073, sig. = 0.000)—showed less bias between estimation of incident  $\{y = 1\}$  and practical observations. The event occurrence is viewed with more possibility when  $P(y)$  is greater than 0.5. As a result, the classification accuracy in Group 0 was 84%, and in Group 1 it was 87.2%. The general accuracy of the prediction was 85.6%. Three variables contributed to the final logistic model and were significant in Wald statistics as in Table 7. The probability distribution of archaeological sites which are related to defensive factors in the landscape is shown in Figure 6.

**Table 7.** Variables in the equation.

	B	S.E	Wals	df	Sig.	Exp (B)	95% C.I. for EXP(B)	
							Lower	Upper
Site_Den	11.054	2.145	26.546	1	0.000	63,205.608	943.035	4,236,267.459
ProxtoRoad	12.901	3.808	11.478	1	0.001	400,730.185	229.897	698,507,800.021
DistoCity	−2.552	0.857	8.873	1	0.003	0.078	0.015	0.418
Constant	−11.464	3.565	10.343	1	0.001	0.000	–	–

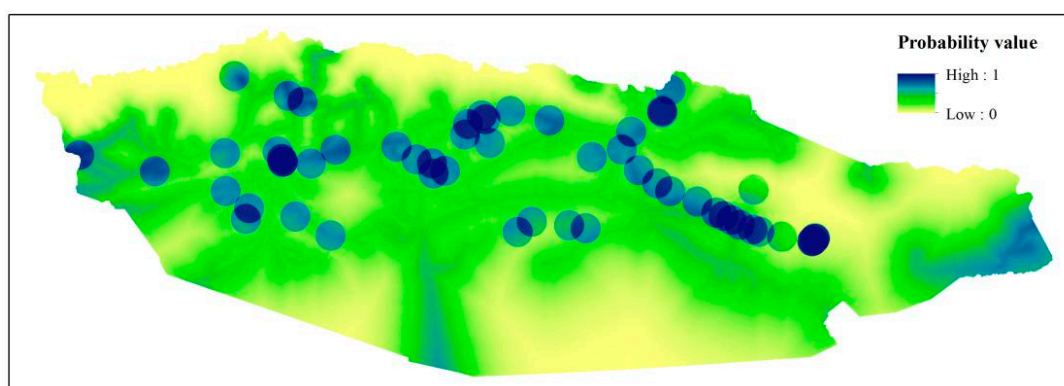
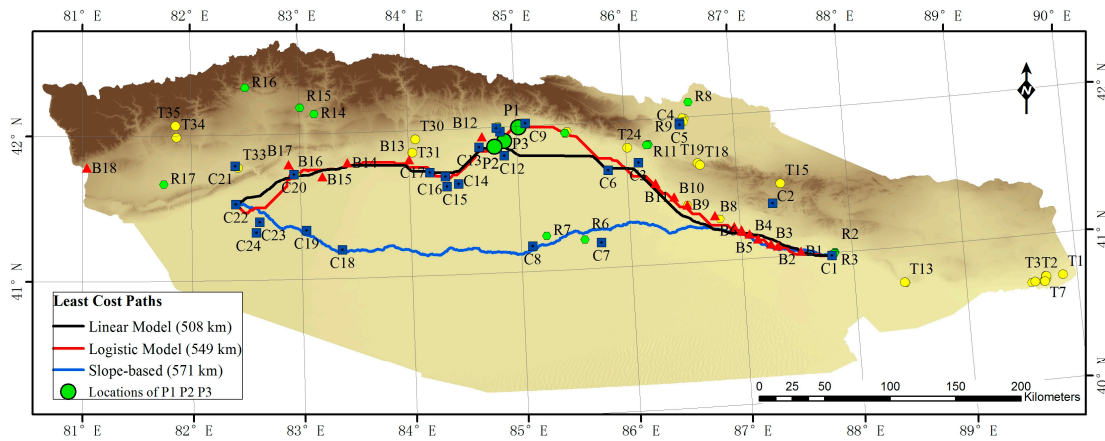


**Figure 6.** Logistic regression of defensive related sites in the Han Dynasty.

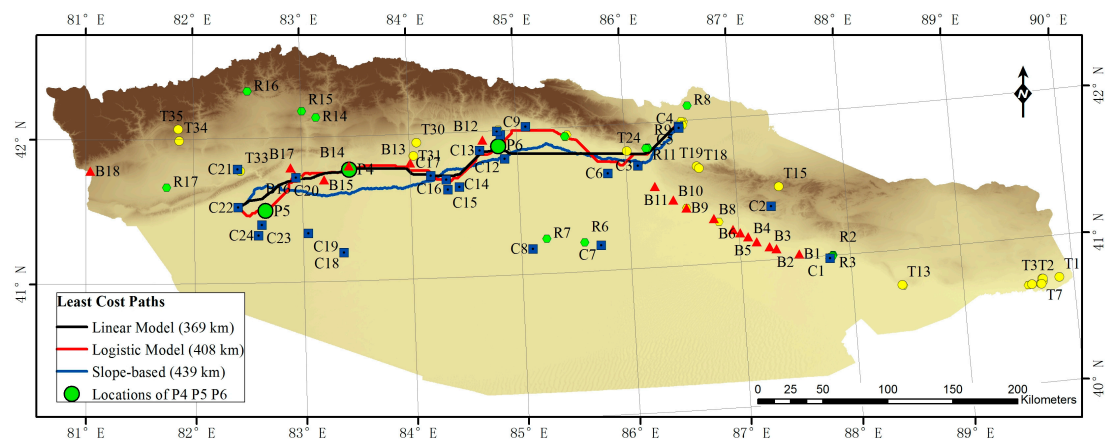
Above all, the effective defensive factors that contribute to the defensibility models are reasonable interpretations of a defensive structure in a landscape. The factor of proximity to road networks had a vital influence on defensibility in both models. Given the z-score of 4.69 in Moran's I auto-correlation analysis of the distance to road network from a site, there is less than 1% likelihood that this clustered pattern could be the result of random chance. This means that the distribution of sites is related to the road system, which coincides with the ancient roads to a certain degree, representing the reciprocity of culture and economy in different areas. Another factor that is important in each model is the distance to the city sites, due to their function of information transmission and territory defense. Moreover, slope is another factor with inverse relation to defensibility, because steep terrain or a mountainous area is difficult for normal marching, thus requiring less defending. However, it is not always like that. Some sites like C2, C21 and B18 are still located in that region in case of emergency and provide deterrent power in the surrounding landscape.

3.4. Least-Cost Paths

Terrain surface has an influence on anthropogenic preference and security strategy for defense, although sometimes the landscape has changed over such a long period [45]. The least-cost path analysis, based on weighted terrain surface, is considered to be a valid method to explore the ancient transportation paths and find an optimal route with minimum cumulative cost from a certain site to another, in practice [39,46]. Particularly, the weighted topography in least-cost analysis has a great impact on the result [47], such that the optimal path may not always follow the Euclidean direction (straight line is the shortest way). The traveling costs are mostly influenced by slope or river networks in terrain surface [48]. Nevertheless, some different cost simulations were verified effectively for rebuilding ancient routes, such as flow direction models and cumulative focal mobility networks [49,50]. The least-cost path analysis is useful to explore cultural communication [51,52]. In this study, the least-cost paths—based on an unusual cost surface weighted with defensive factors in the linear and logistic defensibility models—were used to reconstruct the transportation corridor and are compared with the common least slope cost paths in Figure 7.



(a) from C1 to C22



(b) from C4 to C22

**Figure 7.** Least cost paths based on: linear model, logistic model, and slope model in the direction of (a) from C1 to C22 and the direction of (b) from C4 to C22 (P1, P5: the locations of largest cumulative deviation between the paths of logistic model and slope model; P2, P4: the locations of largest cumulative deviation between the paths of linear model and slope model; P3, P6: the locations of largest cumulative deviation between the paths of linear model and logistic model).

The least-cost path from linear regression analysis is based on the definition of relative importance in defensibility and from the logistic regression analysis is based on probability distribution with optimum defensive conditions. They are different concepts. Yet, the defensibility in the landscape is in direct proportion to the possibility of ancient sites to pass through due to their defensive character. As a result, the least-cost paths were calculated from the linear model that focuses on the differing importance among all archaeological sites, and the logistic model that views all sites as the same occurrence probability. The starting points were chosen as C1 and C4 in different path directions, while C22 is viewed as the destination due to its highest relative importance grade in the west (see Figure 4). This moving from east to west represents the Han Culture propagating to the Western Region. Of course, the inverse traveling direction will not affect the final results.

## 4. Discussions

### 4.1. Defensive Structure

The defensive system of the Han Dynasty is considered as combining the visibility network, transportation paths, and special sites with defensive functions. The statistics in Figure 8 show that the average length of sight lines between beacons in the visibility network is 15.2 km, similar to the average length of 14.4 km between city sites. However, the maximum visibility distance varies. Beacon towers have stronger forewarning and watching ability. Besides, they still have the advantages of low-cost building and high-efficiency signal transmission. As in Figure 9, the strong monitoring ability of each beacon tower is also shown through high cumulative frequency, while the city site focuses on integral associated defensibility, contributing to the surveillance due to the lower cumulative frequency of each site and larger cumulative area observed from the whole city group. In addition, the signal transmission between beacon and city is also an important defensive precaution. It connects the sites with longer linkages for fast signal delivery and constitutes a multifunctional monitoring system.

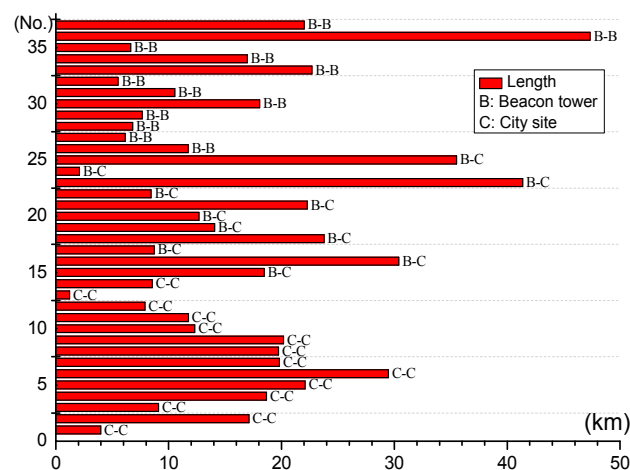


**Figure 8.** Length of visibility lines. The observing sites are classified into three observing types.

The CNA analysis method describes the specific relationship of every single site in the local visibility network. In Region 1 of Figure 3, sites B16, B17, and C20 all have large closeness of CNA measure in the small local visibility network. They also share almost the same high central importance. In other words, the equal importance of the sites means that they are all less important in this simple network. By the analysis of density and inclusivity in Table 3, Region 2 and Region 3 both have a larger redundancy than Region 1, meaning a better social organization network and important defensive regions. This structure has the advantage of stable information exchange to maintain the governance and integral defense. The special site C16 in the local visibility network of Region 2, with the three highest indexes, is explicitly the central site and in the dominant position. It has a strong capacity

to control the information transmission to other sites. The site C12 plays a major role in information control and has a higher centrality level due to high betweenness and degree. Sites B12 and B13 are located in the high value zone in a scatter-plot map in Figure 3, representing strong dominant power for communication to adjacent cities. In this local defensive system, these two beacon towers have the relatively important function of surveillance and control. In Region 3, the beacons align. Particularly from B2 to B7, the visibility lines are combined in a multiple cross pattern that is the result of good visibility and closeness in geographical space, and more importantly, the requirement of a compact observation structure to guard the transportation path. Sites B1, B4, and B7 have an important control function in this local network, while site B11 is beyond visible range from other beacons and acts as an independent tower in the defensive system.

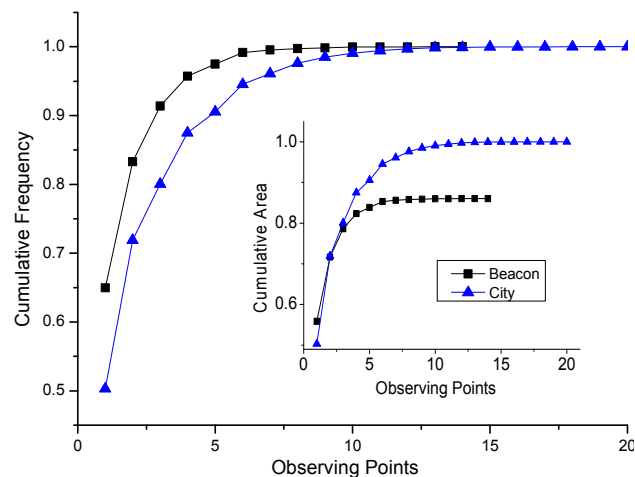


**Figure 9.** Cumulative viewshed of city sites and beacon tower.

#### 4.2. Transportation Corridors

The transportation corridors have an important influence on economic and cultural communication which is controlled by geographical factors and defensive considerations. With the least-cost path analysis that is based on defensibility models, some progress was made to interpret the internal relationship of archaeological sites and some cultural or political connections. The two transportation directions starting from C4 in the orientation of Turpan and from C1 in the orientation of Loulan represent different cultural communication pathways which coincide with the trend of the Silk Road in Han Dynasty [26].

Transportation corridor analysis is compared in the way of cumulative difference that represents the total deviation of two paths during the movement and cumulative difference ratio that delineates the real-time discrepancy proportion in the traveling process. For analysis and validation, 2281 and 1697 sampling points were separately extracted in 200 m intervals in an east-to-west direction along the paths from C1 to C22 and from C4 to C22. As is shown in Figures 7 and 10, the cumulative difference derived from each defensibility model is quite larger than paths from a slope model, which takes the geographical reason as the only influence. The discrepancy varies with different starting points. The two paths from C1 to C22 in linear and logistic models are highly differentiated, with slope-based paths according to the large maximum disparity located at both P1 and P2, in contrast to locations P4 and P5 along the paths from C4 to C22 in linear and logistic models. This is caused by both geographical conditions and regional defensive requirements. With a less cumulative difference from a slope-based route, the paths connecting C4 and C22 do not fit well as those from C1 to C22 in the two defensibility models, because the maximum difference ratio which reflects the variation in the intermediate processing increases to 0.0823 at P6 from 0.0487 at P3. The most different tendency of the paths happens in the section of C6–C11, which is affected by their high probability density based on

the logistic model in its entirety, differentiating with the region of C6–C12 under single-emphasis for defensive importance in the linear model, and the turning points in the traveling progress correspond with the position of C11 and C12 in Figures 7 and 10. The difference ratio is weakened in terms of a long traveling distance from C1 to C22. However, for describing total variation, the average deviation derived from cumulative differences that are assigned to every sampling point along the transportation paths was 2.80 km from C1 to C22, similar to the average deviation of 2.89 km from C4 to C22. It can be concluded that the paths from different defensibility models coincide in general, but with a gap in detail along these corridors.

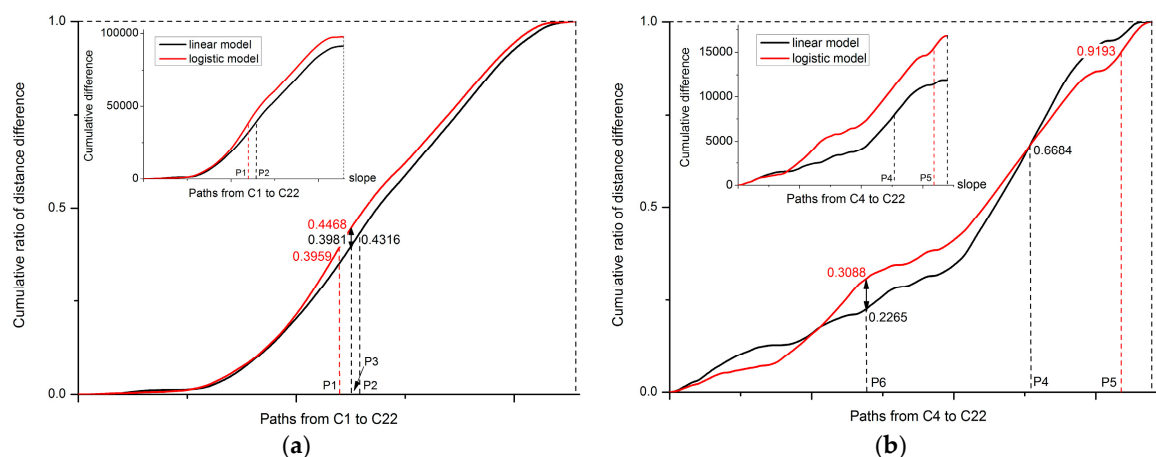


**Figure 10.** Cumulative deviation between defensibility models and slope model.

The transportation corridors play an important role in connecting the Han Empire and the Western Regions. The slope-based paths are obviously different from that based on the defensibility models, especially in the direction of C1 to C22. They are useful to find some inter-relations of the sites, majorly according to the geographical law. The sites C7, C8, C18, C19, C23 that align in the surrounding of the paths are scientifically designed to save physical cost when traveling between them in ancient times. In contrast, the paths from the defensibility model were reconstructed in different ways. They focus more on defensive consideration, not only on the geographical conditions. In the defensibility models, the logistic regression method takes all sites in the study area as an integration with equal importance grade in the defensive system, so the paths would pass through the sites concentrated regions. While the linear regression method is applied by differentiating the defensive importance of each site, so the paths go through the most important site. Some critical sites influence the tendency of the traveling ways, unlike the paths based on geographical factor influencing the location of sites in the slope model. So, the analysis of the defensive role of the important sites is needed.

#### 4.3. Shape Analysis and Defensive Role

Shape analysis aims at discussing cultural patterns and defensive roles in the whole system by an experiential judgment. By general consensus, the square city site in Han Dynasty is from Central Plain Culture, while the round shape is a classic style in the local Western Region [25]. The cultural fusion and military conflict exist as a unit. On the one hand, the culture-related sites signify the communication between each other. On the other hand, the troops were stationed in a fortified site to defend against invasion. Sites C7, C8, C18, C19, and C23 are located along the southern path from C1 to C22 as transfer stations in Figure 7a. Their inherent relations are reflected in shape and structure with the classic character of Han Culture, such as the square shape of C7, C19 and the complicated composition of C18 shown in Figure 11. Sites C8 and C23 are not included in the shape analysis, because the ruin of C8—which the location is inferred from the record of the second heritage census—is not currently visible. Location C23 was investigated in 1954 and recorded as a square city with a length of 69 m from south

to north and 74 m from east to west, which is now disappearing due to occupation by farmland. Site C18, with a large city and special pattern, is considered to be the captain city of cultivating wasteland from the archaeological discovery in early times. So, this transportation path going through these sites is proven influential to cultural communication under the supervisory control of the Han Empire, but its strategic position is not important, as seen by the lack of beacon towers needed in a complete defensive system. In addition, sites C3, C12, C16, C17, and C20 are together considered to guard the key junction connecting east and west along the northern path, based on the slope and defensibility models. Through analysis of shape and structure in Figures 11 and 12, these sites have classic styles of square or irregular polygon shapes, and some with a large mound inside, which manifests the influence of the Central Plain Culture to the West Region (site C20 was the historically famous Qiuci City, the cultural center that was necessary for Silk Road passage, and now is mostly gone except for partial walls in the north ruin, making it unavailable for shape analysis). They are connected in a geographically optimal way for convenient transportation, which greatly contributes to the ancient cultural fusion.

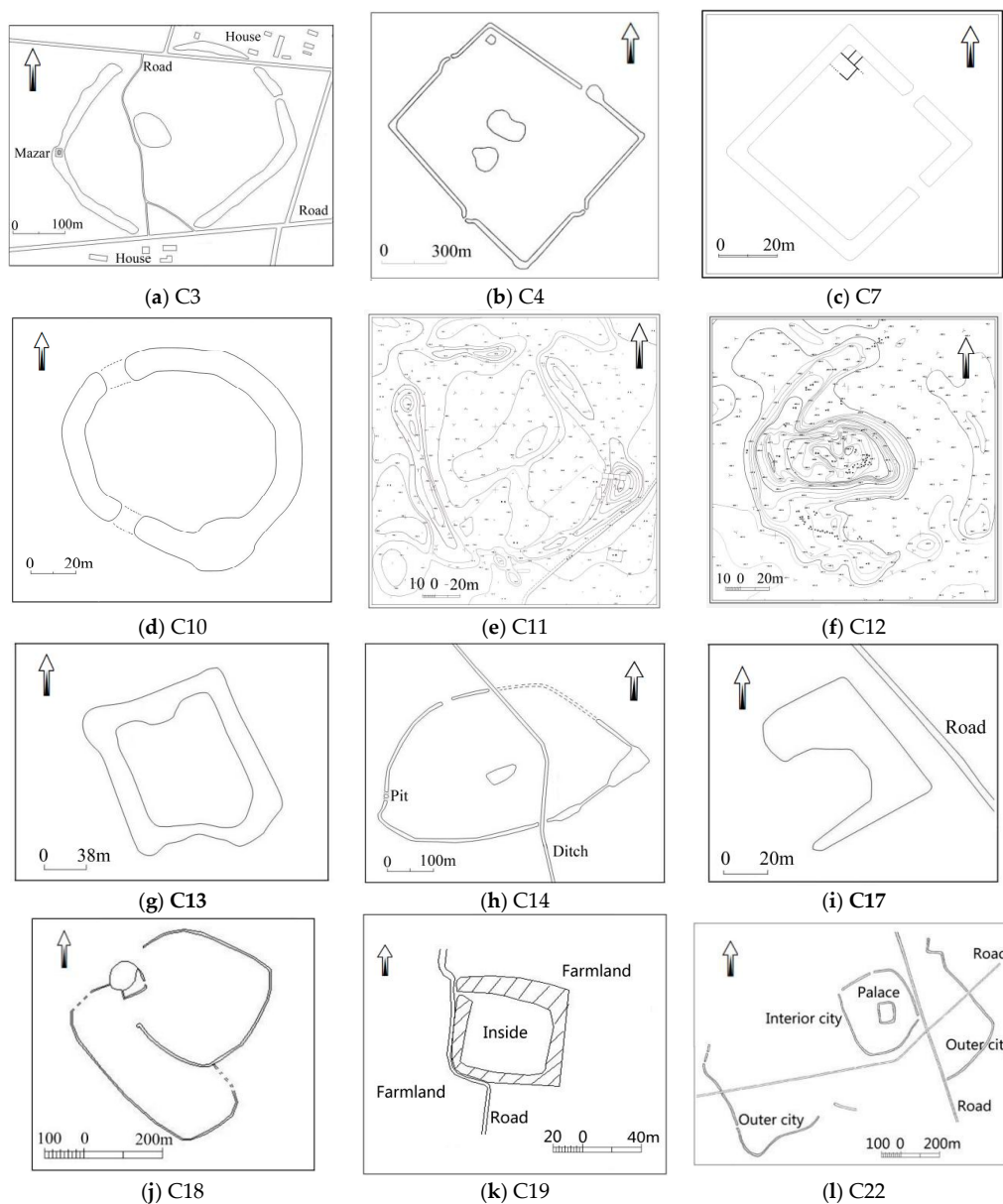


**Figure 11.** Archaeological planar graphs of some city sites with remains on the surface. The materials are from the third cultural relic census data.

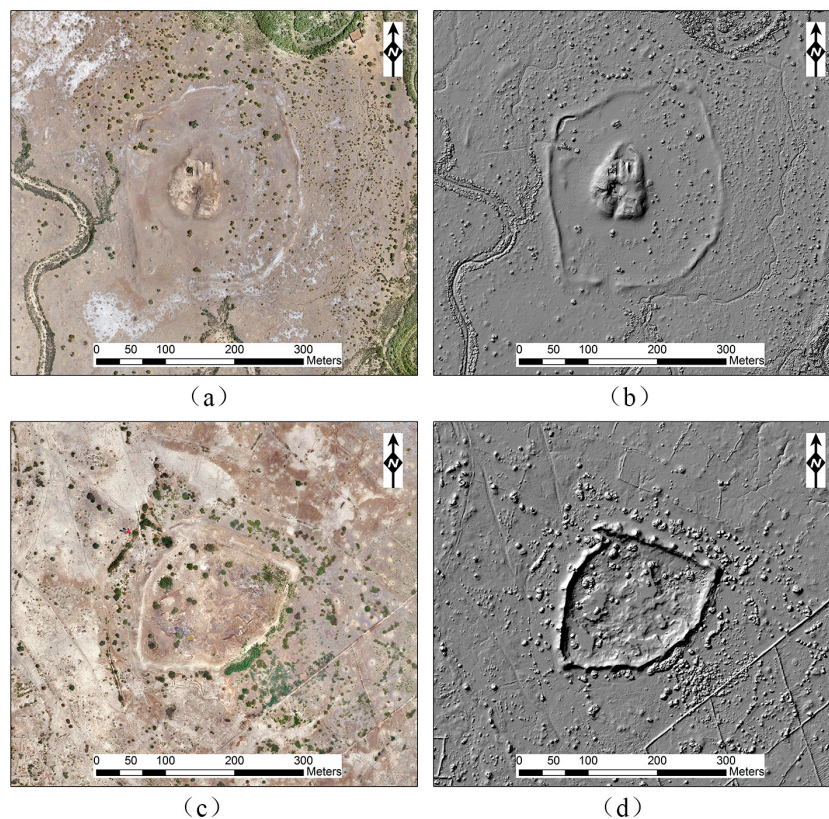


**Figure 12.** (a) Multispectral and (b) hillshade imagery of Kuyux Shahr (C15); (c) Multispectral and (d) hillshade imagery of Kuhne Shahr (C16). They are from aerial photos by unmanned aerial vehicle (UAV) in 2016.

While based on defensibility paths, the city sites C6, C13, as well as beacons B8 to B11 and B13 to B15, also have a great effect on the military activity. Particularly, C6 is destroyed and not able to be judged for the overall shape, but the inevitable traffic place indicates its important role. Site C13 was confirmed as the military castle to guard the transportation corridor, with similar shape and function to C17 (its incomplete square is caused by destruction). The two sites—C13 and C17—are in close relation to the neighboring beacon towers as outposts to defend against attack from the west. Another approximate site, C11, was concluded to be a castle constructed by the Han Empire. Site C10, 4 km away, with a rounder shape, may be the auxiliary city of C11, or the earlier city abandoned after occupation by Han Empire due to its local cultural style in configuration. Along the same path in the east, the site C9, with more than twenty housing ruins, is considered to be for residential living. Its size and shape, however, is difficult to confirm. The cities from C9 to C13 form a linear defensive and residential group together with beacon B12.

Another group, with four sites from C14 to C17 in the central position, constitutes a cooperative defensive unit to guard transportation lines. As a dominant site to control information exchange in the visibility network, C16 also has a high structural hierarchy with anomalous shape and quite large scale. It has 22 horse-faces (the city defense facility in the walls in ancient China against side attack) along the city wall, shown in Figures 12 and 13b. The defensive role is obvious. Only 8 km away in the south, C15 is another high-grade city whose shape is between round and square and with a large mound inside (see Figure 13a). Sites C15 and C16 meet some criteria of the Western Region's Frontier Command in the following aspects: high defensive importance, vital location along the transportation lines, large scale, and classic architectural shape of the Han Culture. As well, site C17, as a military castle, guarded the west of Luntai, and C14 may be the ancient satellite city or captain city for cultivating wasteland and providing logistical supplies with lower defensive importance in

spatial position, in spite of its large dimension. What should be noted is that the mound in the east side of C14 could provide far horizon to defend against invasion from the east. Site C14 is the first gate to pass through when traveling further west. It can be inferred that this region had cooperative defense and prospered during the Han Dynasty for these intensive sites.



**Figure 13.** (a) The large mound inside the site of Kuyux Shahr city with an 8-meter height; (b) the corner of the site Kuhne Shahr in the north-west with a horse-face for defending attack.

In the field investigation, more archaeological details were acquired about C15 and C16. In the city site C15, the commanding height of the large mound in city and its adobe buildings prove the local authority controlling the whole city. The burning indications of the ancient buildings inside the city are proof of being destroyed from warfare. This site is considered an unidentified official institution or kingdom in the Western Region. Many remains inside C16 were found, including numerous pottery shards, iron slag, and coins, demonstrating frequent human activities and important residential and military roles. It was governed by the Han Empire. By the comprehensive analysis of defensive function and field investigation, the important historical roles of the two sites were verified by these archaeological characteristics.

Through this research, some defensive roles of sites along the transportation corridors have been confirmed, though the paths based on defensibility analysis in the Han Dynasty still need more verification. It affords researchers feasible methods to analyze the organizational pattern of the archaeological sites and find ancient transportation corridors. These corridors are useful to confirm the cultural connections and provide reference to discover unknown ancient routes. The defensibility distributions of both the linear and logistic regression models can be recognized as efficient cost surfaces to explore optimal routes under cultural and political purposes. The military defensive system is also represented, with the visibility network constituted by special sites. More verification from archaeological information will be helpful to explain specific internal cultural relationships. As recorded in documentation, the Han Empire opened up wasteland and built the Western Region's Frontier Command to govern the early Xinjiang and protect the Silk Road from invasion by the Huns. These discussions can provide some clues to locate the Western Region's Frontier Command of the Han Dynasty among important sites and find the missing beacons along the Silk Road in major defence area. The ancient paths were also simulated in another way, based on the slope model. They are considered to be the early routes before large numbers of sites were built to guard the Silk Road. When defensive requirements became important, the paths transferred to other ways with maximum defensive importance in the landscape or high-probability density places with site clustering. The least physical cost is a basic consideration for matching or traffic at any time, so the slope-based path is an alternative option. The transportation line in the south of the study area goes along the river basin of Tarim, and thus is easily affected by changes in the watercourse. The historical correlation between path transition and environmental variation is worthy of more discussion in the future.

## 5. Conclusions

In this research, the defensive system in the Han Dynasty, which is directly associated with military authority in the governed area of the southern Tianshan Mountains in Central Xinjiang, was rebuilt using SRTM DEM. In history, the military authority of the Han Empire contributed to the prosperity and stability along the Silk Road. By constructing the compound visibility network and simulating transportation corridors based on the quantified defensibility model, the defensive function of ancient sites was discussed together with the pattern of their information transmission and cultural communication. The analysis results show that the visibility network constituted three local parts, two of which in the east are the important defensive regions. The beacons with stronger observing ability play a more important role in this network. The conspicuous defensive functions are mainly reflected in the eight city sites (Uzgen Bulak, Shah Kalandar, Agra, Chuck Castle, Kuyux Shahr, Kuhne Shahr, Caladar and Qiuci) and some Beacons (Turkish, Caleta, Akeerdick, Karaya, West Layisu, QiuFutur, and Dunmaili Tur). Respectively speaking, the sites of Agra and Kuhne Shahr were proven to have more controlling ability in their local defensive region in a visibility network. They have important effects on the surveillance and governance of the transportation corridors. The sites of Kuyux Shahr and Kuhne Shahr have been confirmed as significant in the defensive system as the alternative site of the Western Region's Frontier Command through defensibility and shape analysis. Meanwhile, the southern sites (Chalcedo Ursa, Kajaskule, Big city, Aksi and Tashton) may serve as military stations and residential cities along the slope-based path and Tarim River valley. The route passing through these southern sites had less defensive importance during the Han Dynasty because no strategic beacons in that area can combine to form a comprehensive defensive system. In addition, the transportation corridors based on the linear defensibility model fit well with that based on the logistic regression method, in general. They were the main historical defensive transportation corridors. The southern least-cost path, based on a slope model, differs greatly with other paths from Yingpan to Muscat. It provided an optional traffic path with less defensive requirements and played a less important role in cultural communication after the Silk Road was opened. All the paths constitute the main arterial traffic in the Han Dynasty.

The reconstructed defensive system in this research shows the different defensive roles of the ancient sites and possible transportation lines for military activity or cultural communication. It can be applied to provide some insights into social organization and human behavior preference under defensive considerations. Furthermore, using this methodological framework, the spatial connotation of ancient sites can be explored, and anthropological archaeology can be recognized more broadly. More meaningful work in the future is needed, such as seeking out the Western Region's Frontier Command or the lost beacon towers along the Silk Road. The conclusions from the defensive system analysis are expected to be verified by the some more archaeological discoveries.

**Supplementary Materials:** The SRTM DEM data set was provided by the International Scientific & Technical Data Mirror Site, Computer Network Information Center, the Chinese Academy of Sciences, <http://www.gscloud.cn>.

**Acknowledgments:** This research is funded by the national key technology R & D program of the project "Research on the Application of Remote Sensing Technology in Exploring the Origin of Chinese Civilization" (No. 2013BAK08B06) and "Remote sensing and geophysical comprehensive in archaeological research of China classical archaeological site" (No. 2015BAK01B01). We sincerely thanks Luntai administration of cultural heritage, Huarui Zhang and the staff of Luntai museum in Xinjiang. We also thank Xinjiang Cultural Relics and Archaeology Institute and the staff for providing the data of archaeological sites, especially Jianjun Yu, Xingjun Hu for giving advises of archaeological analysis and Zhihao Dang for providing help for field investigation.

**Author Contributions:** J.Z. Contributed to the article writing and experiment. F.L. and H.G. analyzed the archaeological data and the historical document. Y.N. and L.Y. designed the study methods.

**Conflicts of Interest:** The authors declare no conflicts of interest.

## Appendix A

Table A1. Archaeological site comparison table.

Yingpan (C1)	Shahr Tokai (C2)	Uzgen Bulak (C3)	Bogurda (C4)	Tacroli (C5)	Shah Kalandar (C6)
Chalcedo Ursa (C7)	Kajaskule (C8)	Yeyungou Mazar (C9)	Aziz (C10)	Wuliponk (C11)	Agra (C12)
Chuck Castle (C13)	Drow Kurt (C14)	Kuyux Shahr (C15)	Kuhne Shahr (C16)	Caladar (C17)	Big city (C18)
Aksi (C19)	Qiuci (C20)	Kuonaxiehair (C21)	Muscat (C22)	Tashton (C23)	Egmery Ruddock (C24)
Turkish (B1)	West Turkish (B2)	Keyak Kuduk (B3)	Caleta (B4)	Gumush (B5)	Saluwak (B6)
Akeerdick (B7)	Saqit (B8)	Sunji (B9)	Ark Shimron (B10)	Sukati (B11)	Karaya (B12)
West Layisu (B13)	QiuFutur (B14)	Dunmaili Tur (B15)	KuokongBazi (B16)	Kezier Garha (B17)	Yabuyi (B18)

## References

- Abdukirim, M. On the troops wasteland-opening up and its effect in the western regions during the Han-Tang Dynasty. *J. Kashgar Teach. Coll.* **2010**, *31*, 46–49. [[CrossRef](#)]
- Jiang, N. Research on the System of Frontier in Han Dynasty. Ph.D. Thesis, Central China Normal University, Wuhan, China, 2013.
- Song, C. Establishment of the Western Regions Frontier Command and Competition for Qiuci between Han Empire and Huns during the Western and Eastern Han, analyzing from Wulei to Tagan. *Qiuci Stud.* **2012**, *5*, 58–72.
- Zhou, H. Jurisdiction and management of Han and Tang Dynasty in Xinjiang from the archaeological data. *J. Xinjiang Norm. Univ.* **2000**, *21*, 40–49. [[CrossRef](#)]
- Zhang, A.F.; Tian, H.F. The remains of the site and the layout of the defense cities of the Han Dynasty in the Western Regions. *J. Chin. Hist. Geogr.* **2015**, *30*, 47–55.
- Garcia-Moreno, A. To see or to be seen...is that the question? An evaluation of palaeolithic sites' visual presence and their role in social organization. *J. Anthropol. Archaeol.* **2013**, *32*, 647–658. [[CrossRef](#)]
- Rua, H.; Goncalves, A.B.; Figueiredo, R. Assessment of the Lines of Torres Vedras defensive system with visibility analysis. *J. Archaeol. Sci.* **2013**, *40*, 2113–2123. [[CrossRef](#)]
- Déderix, S. A matter of scale. Assessing the visibility of circular tombs in the landscape of Bronze Age Crete. *J. Archaeol. Sci. Rep.* **2015**, *4*, 525–534. [[CrossRef](#)]
- Ogburn, D.E. Assessing the level of visibility of cultural objects in past landscapes. *J. Archaeol. Sci.* **2006**, *33*, 405–413. [[CrossRef](#)]
- Sevenant, M.; Antrop, M. Settlement models, land use and visibility in rural landscapes: Two case studies in Greece. *Landscape Urban Plan.* **2007**, *80*, 362–374. [[CrossRef](#)]
- Kyle Bocinsky, R. Extrinsic site defensibility and landscape-based archaeological inference: An example from the Northwest Coast. *J. Anthropol. Archaeol.* **2014**, *35*, 164–176. [[CrossRef](#)]
- Martindale, A.; Supernant, K. Quantifying the defensiveness of defended sites on the Northwest Coast of North America. *J. Anthropol. Archaeol.* **2009**, *28*, 191–204. [[CrossRef](#)]
- Danese, M.; Masini, N.; Biscione, M.; Lasaponara, R. Predictive modeling for preventive archaeology: Overview and case study. *Cent. Eur. J. Geosci.* **2014**, *6*, 42–55. [[CrossRef](#)]
- Carrer, F. An ethnoarchaeological inductive model for predicting archaeological site location: A case-study of pastoral settlement patterns in the Val di Fiemme and Val di Sole (Trentino, Italian Alps). *J. Anthropol. Archaeol.* **2013**, *32*, 54–62. [[CrossRef](#)]
- Turrero, P.; Domínguez-Cuesta, M.J.; Montserrat Jiménez-Sánchez, M.; García-Vázquez, E. The spatial distribution of Palaeolithic human settlements and its influence on palaeoecological studies: A case from Northern Iberia. *J. Archaeol. Sci.* **2013**, *40*, 4127–4138. [[CrossRef](#)]
- Jaroslawa, J.; Hildebrandt-Radke, I. Using multivariate statistics and fuzzy logic system to analyse settlement preferences in lowland areas of the temperate zone: An example from the Polish Lowlands. *J. Archaeol. Sci.* **2009**, *36*, 2096–2107. [[CrossRef](#)]
- Garcia, A. GIS-based methodology for Palaeolithic site location preferences analysis. A case study from Late Palaeolithic Cantabria (Northern Iberian Peninsula). *J. Archaeol. Sci.* **2013**, *40*, 217–226. [[CrossRef](#)]
- Ullah, I. A GIS method for assessing the zone of human-environmental impact around archaeological sites: A test case from the Late Neolithic of Wadi Ziqlâb, Jordan. *J. Archaeol. Sci.* **2011**, *38*, 623–632. [[CrossRef](#)]
- Jones, E.E. An analysis of factors influencing sixteenth and seventeenth century Haudenosaunee (Iroquois) settlement locations. *J. Anthropol. Archaeol.* **2010**, *29*, 1–14. [[CrossRef](#)]

20. Moskal-del Hoyo, M.; Litynska-Zajac, M.; Korczynska, K.; Cywa, K.; Kienlin, T.L.; Cappenberg, K. Plants and environment: Results of archaeobotanical research of the Bronze Age settlements in the Carpathian Foothills in Poland. *J. Archaeol. Sci.* **2015**, *53*, 426–444. [[CrossRef](#)]
21. Menze, B.H.; Ur, J.A. Mapping patterns of long-term settlement in Northern Mesopotamia at a large scale. *Proc. Natl. Acad. Sci. USA* **2012**, *778*–787. [[CrossRef](#)] [[PubMed](#)]
22. Canosa-Betés, J. Border surveillance: Testing the territorial control of the Andalusian defense network in center-south Iberia through GIS. *J. Archaeol. Sci. Rep.* **2016**, *9*, 416–426. [[CrossRef](#)]
23. Lanen, R.J.; Kosian, M.C.; Groenewoudt, B.J.; Spek, T.; Jansma, E. Best travel options: Modeling Roman and early-medieval routes in the Netherlands using a multi-proxy approach. *J. Archaeol. Sci. Rep.* **2015**, *3*, 144–159. [[CrossRef](#)]
24. Fletcher, R. Some spatial analyses of Chalcolithic settlement in Southern Israel. *J. Archaeol. Sci.* **2008**, *35*, 2048–2058. [[CrossRef](#)]
25. Lin, M.C. Research on today's location of Regions Frontier Command site from archaeological perspective. *Hist. Res.* **2013**, *6*, 43–58.
26. Xinjiang Bureau of Surveying Mapping and Geoinformation. *The Map of China Xinjiang*, 1st ed.; Sino Maps Press: Beijing, China, 2015; pp. 6–9.
27. Zhou, J. Study on the Xiyu Duhu of the Western Han Dynasty. Master's Thesis, Northwest Normal University, Lanzhou, China, 2010.
28. Hong, T. A brief comment on the research on the safeguard city in the Western Region in Han Dynasty. *J. Xinjiang Norm. Univ.* **2007**, *28*, 5–10. [[CrossRef](#)]
29. Shang, Y.B. Several economical problems of Qiuci in Han and Tang Dynasty. *J. Xinjiang Norm. Univ.* **1989**, *4*, 31–37.
30. Hu, Z.H.; Peng, J.W.; Hou, Y.L.; Shan, J. Evaluation of Recently Released Open Global Digital Elevation Models of Hubei, China. *Remote Sens.* **2017**, *9*, 1–16. [[CrossRef](#)]
31. Fisher, P.; Farrelly, C. Spatial Analysis of visible areas from the Bronze Age Cairns of Mull. *J. Archaeol. Sci.* **1997**, *24*, 581–592. [[CrossRef](#)]
32. Scott, J. *Social Network Analysis: A Handbook*, 3rd ed.; Sage Publications: London, UK, 2012; pp. 32–97.
33. Wasserman, S.; Faust, K. Social network analysis in the social and behavioral sciences. In *Social Network Analysis Methods and Application*, 1st ed.; Cambridge University Press: Cambridge, UK, 1994; pp. 3–27.
34. Earley-spadoni, T. Landscapes of warfare: Intervisibility analysis of Early Iron and Urartian fire beacon stations (Armenia). *J. Archaeol. Sci. Rep.* **2015**, *3*, 22–30. [[CrossRef](#)]
35. De Montis, A.; Caschili, S. Nuraghes and landscape planning: Coupling viewshed with complex network analysis. *Landscape Urban Plan.* **2012**, *105*, 315–324. [[CrossRef](#)]
36. Mullins, P. Webs of defense: Structure and meaning of defensive visibility networks in Prehispanic Peru. *J. Archaeol. Sci. Rep.* **2016**, *8*, 346–355. [[CrossRef](#)]
37. Wikipedia. Available online: <https://en.wikipedia.org/wiki/Centrality> (accessed on 4 November 2016).
38. De Reu, J.; Bourgeois, J.; De Smedt, P.; Zwertvaegher, A.; Antrop, M.; Bats, M.; De Maeyer, P.; Finke, P.; Van Meirvenne, M.; Verniers, J.C.; et al. Measuring the relative topographic position of archaeological sites in the landscape, a case study on the Bronze Age barrows in northwest Belgium. *J. Archaeol. Sci.* **2011**, *38*, 3435–3446. [[CrossRef](#)]
39. Siart, C.; Eitel, B.; Panagiotopoulos, D. Investigation of past archaeological landscapes using remote sensing and GIS: A multi-method case study from Mount Ida, Crete. *J. Archaeol. Sci.* **2008**, *35*, 2918–2926. [[CrossRef](#)]
40. Marsh, E.J.; Schreiber, K. Eyes of the empire: A viewshed-based exploration of Wari site-placement decisions in the Sondondo Valley, Peru. *J. Archaeol. Sci. Rep.* **2015**, *4*, 54–64. [[CrossRef](#)]
41. Falconer, L.; Hunter, D.C.; Telfer, T.C.; Ross, L.G. Visual, seascape and landscape analysis to support coastal aquaculture site selection. *Land Use Policy* **2013**, *34*, 1–10. [[CrossRef](#)]
42. Fernandes, R.; Geeven, G.; Soetens, S.; Klontza-Jaklova, V. Deletion/Substitution/Addition (DSA) model selection algorithm applied to the study of archaeological settlement patterning. *J. Archaeol. Sci.* **2011**, *38*, 2293–2300. [[CrossRef](#)]
43. Perakis, K.; Moysiadis, A. Geospatial predictive modeling of the Neolithic archaeological sites of Magnesia in Greece. *Int. J. Digit. Earth* **2011**, *4*, 421–433. [[CrossRef](#)]
44. Espa, G.; Benedetti, R.; De Meo, A.; Ricci, U.; Espa, S. GIS based models and estimation methods for the probability of archaeological site location. *J. Cult. Herit.* **2006**, *7*, 147–155. [[CrossRef](#)]

45. Carballo, D.M.; Pluckhahn, T. Transportation corridors and political evolution in highland Mesoamerica: Settlement analyses incorporating GIS for northern Tlaxcala, Mexico. *J. Anthropol. Archaeol.* **2007**, *26*, 607–629. [[CrossRef](#)]
46. Sakaguchi, T.; Morin, J.; Dickie, R. Defensibility of large prehistoric sites in the Mid-Fraser region on the Canadian Plateau. *J. Archaeol. Sci.* **2010**, *37*, 1171–1185. [[CrossRef](#)]
47. Lanen, R.J.; Kosian, M.C.; Groenewoudt, B.J.; Jansma, E.; Rowin, J.; Menne, C.; Bert, J.; Esther, J. Finding a way: Modeling landscape prerequisites for Roman and early-Medieval routes in the Netherlands. *Geoarchaeology* **2015**, *30*, 200–222. [[CrossRef](#)]
48. Güimil-Farina, A.; Parceró-Oubina, C. “Dotting the joins”: A non-reconstructive use of least cost paths to approach ancient roads. The case of the Roman roads in the NW Iberian Peninsula. *J. Archaeol. Sci.* **2015**, *54*, 31–44. [[CrossRef](#)]
49. Fábrega-Álvarez, P. Moving without destination. A theoretical, GIS-based determination of routes (optimal accumulation model of movement from a given origin). *Archaeol. Comput. Newsl.* **2006**, *64*, 7–11.
50. Llobera, M.; Fábrega-Álvarez, P.; Parceró-Oubiña, C. Order in movement: A GIS approach to accessibility. *J. Archaeol. Sci.* **2011**, *38*, 843–851. [[CrossRef](#)]
51. Field, J.S.; Petraglia, M.D.; Lahr, M.M. The southern dispersal hypothesis and the South Asian archaeological record: Examination of dispersal routes through GIS analysis. *J. Anthropol. Archaeol.* **2007**, *26*, 88–108. [[CrossRef](#)]
52. Yubero-Gómez, M.; Rubio-Campillo, X.; Javier López-Cachero, F.; Esteve-Gràcia, X. Mapping changes in late prehistoric landscapes: A case study in the northeastern Iberian Peninsula. *J. Archaeol. Sci.* **2015**, *40*, 123–134. [[CrossRef](#)]



© 2017 by the authors. Licensee MDPI, Basel, Switzerland. This article is an open access article distributed under the terms and conditions of the Creative Commons Attribution (CC BY) license (<http://creativecommons.org/licenses/by/4.0/>).